scientific reports

Check for updates

OPEN

Composition formulas of solid-solution alloys derived from chemical-short-range orders

Zhuang Li[1], Dandan Dong[2]✉, Lei Zhang[3], Shuang Zhang[4], Qing Wang[1] & Chuang Dong[1,4]

Solid solutions are the basis for most industrial alloys. However, the relationships between their characteristic short-range orders and chemical compositions have not been established. The present work combines Cowley parameter α with our cluster-plus-glue-atom model to accurately derive the chemical units of binary solid-solution alloys of face-centered cubic type. The chemical unit carries information on atomic structure and chemical composition, which explains prevailing industrial alloys. For example, chemical units in $Cu_{68.9}Zn_{31.1}$ alloy with $\alpha_1 = -0.137$ are formulated as $[Zn\text{-}Cu_{10}Zn_2]Zn_2Cu_2$ and $[Zn\text{-}Cu_{10}Zn_2]Zn_3Cu_1$, with 64.0–70.0 wt% Cu corresponding to the most widely used cartridge brass C26000 (68.5–71.5 Cu). This work answers the long-standing question on the composition origin of solid-solution-based industrial alloys, by tracing to the molecule-like chemical units implied in chemical short-range ordering in solid solutions.

In one of the early review on solid solutions in 1925, Bruni[1] raised a preliminary question: does the chemical molecule continue to exist in the crystalline state? This question looks quite naive at present but must be answered in his time as most of the metals are based on solid solutions and they all have specific chemical compositions, just like any molecular substance whose chemistry is contained in the molecular structure. The first results of X-ray analyses by Bragg[2] answered this question in the negative, by affirming that within the crystal edifice only atoms exist and the molecule vanishes into the lattice. However, the structural origin of chemical compositions of industrial alloys remains open. The key to understanding the composition mystery must lie in the structure of solid solutions, which has been a hot topic in the early twentieth century. Bragg and Williams were among the first to propose a statistical model that considers the order and disorder in solid solutions as a co-operative long-range phenomenon[3]. This model was then extended to a more elaborated theory by Bethe[4], assuming the short-range interaction in nearest neighborhood. The long- and short-range orders are well unified in Cowley's[5] short-range order parameters α_i, expressing the interaction of a given atom A with the atoms of the ith shell of atoms surrounding it:

$$\alpha_i = 1 - \frac{n_i}{m_B c_i} \tag{1}$$

where n_i is the number of B atoms among the c_i atoms of the ith shell, and m_B is the mole fraction of B atoms in A–B binary alloy. Equations for the long-range order parameter of Bragg and Williams are obtained by considering the limiting case of i very large. Since then it is well recognized that short-range ordering is the major structural feature of solid solutions.

In an effort to explore the composition origin implied in such ordered and disordered local structures, our team has been engaged in developing a so-called cluster-plus-glue-atom model[6–8] which simplifies any short-range order into a local unit covering a nearest-neighbor cluster plus a few next-neighbor glue atoms, expressed in cluster formula form as [cluster](glue atoms). This structural unit, showing charge neutrality and mean density following Friedel oscillation[9], resembles in many ways chemical molecules and henceforth is termed 'chemical unit'[7]. The only difference from common concept of molecule lies in the way the chemical units are separated: instead of relatively weak inter-molecular forces between molecules, here the chemical units are linked by chemical bonding. We have shown by analyzing many industrial alloys that popular alloys are all based on

[1]Key Laboratory for Materials Modification by Laser, Ion and Electron Beam (Dalian University of Technology), Ministry of Education, Dalian 116024, China. [2]College of Physical Science and Technology, Dalian University, Dalian 116622, China. [3]Science and Technology on Surface Physics and Chemistry Laboratory, Mianyang 621907, China. [4]School of Materials Science and Engineering, Dalian Jiaotong University, Dalian 116028, China. ✉email: dandan3006@126.com

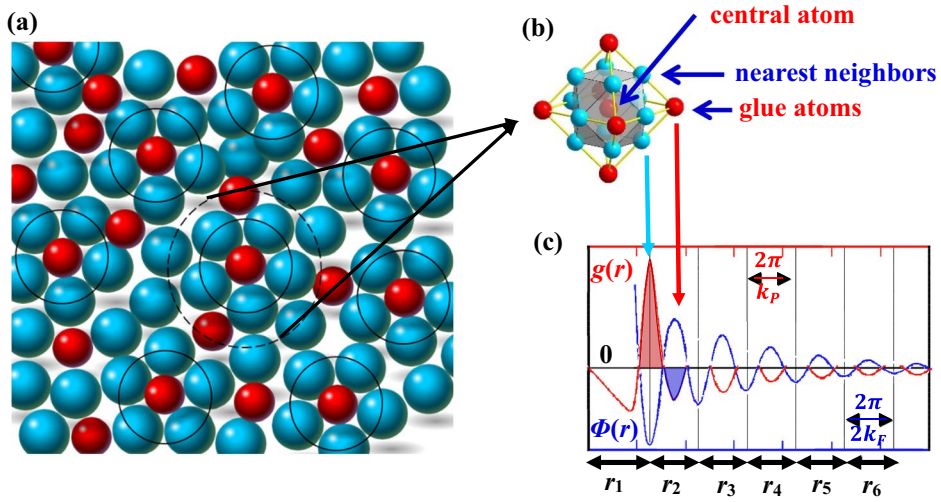

Figure 1. (**a**) Schematic diagram of short-range order and long-range disorder distribution of solute atoms in binary solid solution alloys. (**b**) Cluster configuration of binary FCC structure. (**c**) Idealized pair distribution function $g(r)$ and total potential energy $\Phi(r)$ curve felt by electrons[12].

simple cluster-plus-glue-atom formulas, such as $[Zn\text{-}Cu_{12}]Zn_4$ for Cu-30Zn, $[Ni\text{-}Fe_{12}]Cr_2$(Ni,Nb,Ti) for maraging stainless steel Custom465, etc.[7].

However, despite of the proved capacity of the cluster-plus-glue-atom model in interpreting composition origins of alloys, there is an obvious gap between the idealized formulas (e.g., the nearest neighbors are always fully occupied by solvent atoms such as $[Zn\text{-}Cu_{12}]Zn_4$) and the real chemical short-range ordering (the nearest neighbors are always mixed-occupied) that can be measured, for example using parameter α_i. The α_i parameter describes the statistical deviation from the average alloy composition in each redial shell. The composition deviation appears most prominently in the first and second nearest neighbors, which agrees perfectly with the picture of the cluster-plus-glue-atom model that covers also the same radial range. The present work is our first attempt to fill in the gap, by showing how to relate the measurable parameters α_i, within the framework of the cluster-plus-glue-atom model, to the construction of composition formulas of typical binary solid solution alloys with face-centered cubic (FCC) structure.

Theoretical methods

We first briefly review the fundamentals that lead to chemical units, as fully detailed in reference[7]. Short-range ordering is formed due to the charge shielding around any given atom that produces oscillating distribution of electron density, namely Friedel oscillations[10,11]. As shown in Fig. 1c, the total potential function $\Phi(r) \propto -\sin(2k_F r)/r^3$ felt by the electrons at radial distance r periodically decays with the third power of r, where k_F is Fermi wave vector. This oscillating behavior of electrons in turn causes the same oscillation of atomic density $g(r)$ in the real space, which is prominent in short r range, especially at the nearest and next-nearest neighborhoods. A local chemical unit is defined using a charge-neutral cut-off distance of $1.76\lambda_{Fr}$, $\lambda_{Fr} = \pi/k_F$ being Friedel wavelength, that encloses the nearest-neighbor cluster and a few next-neighbor glue atoms. For FCC structure, its cluster-plus-glue-atom model is shown in Fig. 1b, the cluster is cuboctahedron with coordination number of 12 and the glue-atom shell in the next neighborhood is octahedron of coordination 6. A solid solution is then regarded as the random packing of such units as schematically illustrated in Fig. 1a. The chemical unit of a binary A–B system is expressed in cluster formula form as $[A\text{-}M_{12}]A_xB_y$, where $M_{12} = B_{n1}A_{12-n1}$ refers to the average of nearest-neighbor atoms and integer $x+y$ represents the number of glue atoms with $0 < x+y < 6$.

Following[13], the chemical unit volume is the sum of the each atomic volume $\left[(1+x)\cdot R_A^3 + 12\cdot R_M^3 + y\cdot R_B^3\right]\cdot(4\pi/3)/0.74$, where R's are atomic radii and 0.74 is the packing efficiency of FCC structure. This volume is also equal to the spherical volume enclosed by the charge-neutral cut-off distance $1.76\lambda_{Fr}$, $(4\pi/3)\cdot(1.76\lambda_{Fr})^3$. Since $R_A + R_M = 1.25\,\lambda_{Fr}$ is the nearest-neighbor distance, the x–y relationship is obtained:

$$x\cdot R_{A/M}^3 + y\cdot R_{B/M}^3 \approx 2\cdot(R_{A/M}+1)^3 - 12 - R_{A/M}^3 \tag{2}$$

where $R_{A/M}$ and $R_{B/M}$ are respectively the ratios of R_A and R_B over $R_M = (n_1\cdot R_B + (12-n_1)\cdot R_A)/12$. Goldschmidt radii of atoms are generally adopted. When $R_A = R_B$, $x+y=3$, which means a 16-atom cluster formula for an FCC solid solution composed of solute and solvent atoms of equal atomic radii, or $[A\text{–}B_{12}](A,B)_3$.

As demonstrated in references[7,14,15], compositions of commonly used industrial alloys such as Cu alloys, Al alloys, stainless steels, and Ni-based superalloys fall close to the model predictions, validating the presence of simple chemical units in metallic alloys and the generality of the cluster formulism. Our recent work[16] shows that the model also applies in high-entropy alloys, after appropriate elemental classification. The solid solutions

of hexagonal closed-packed type can be treated similarly, as it shows the same coordination number of 12 (the nearest-neighbor cluster is twinned octahedron) and is also close-packed. The body-centered cubic structure, featuring a rhombododecahedral cluster with a coordination number of 14 and a non-close-packing, should be dealt with separately, which is an on-going work.

Now we show the two basic procedures towards constructing the chemical unit with formula $[A–B_{n1}A_{c1\text{-}n1}]A_xB_y$ using the short-range-order parameter α_1.

(1) Determination of nearest-neighbor atoms using α_1

For a given alloy with a known B's atomic fraction m_B and coordination number c_1, the number of B atoms in the nearest-neighbor shell, n_1, is directly obtained by using the measured α_1 value following Eq. (1):

$$n_1 = m_B \cdot c_1 \cdot (1 - \alpha_1) \tag{3}$$

The n_1 value should be approximated into a nearby integer. When the short-range-order parameter α_1 is negative, the integer is the roundup of n_1, for B atoms tend to be enriched in the nearest neighbor shell due to the attractive interaction mode between the central A and neighboring B atoms. Alternative, when α_1 is positive, the integer is the rundown of n_1.

(2) Calculation of next-neighbor glue atoms via Eq. (2)

By introducing into Eq. (2) the atomic ratios $R_{A/M}$ and $R_{B/M}$, the relationship between x and y is established. This relationship should also agree with the alloy composition, i.e., $(n_1 + y)/(1 + c_1 + x + y) = m_B$. For FCC, the ($x$, y) solution is also limited to $0 < x + y < 6$. A unique set of (x, y) solution is then possible, from which two sets of close-integers are obtained, so that the measured alloy composition falls between the two chemical units.

These procedures will be detailed in analyzing typical examples of popular binary copper alloys in the next.

Examples of binary Cu alloys

Cu-30Zn alloy. Though industrial Cu–Zn binary alloys cover a Zn range up to ~ 40 wt%, Cu-30Zn, or cartridge brass, is the most widely used grade. The α_i parameters reaching a few tens of shells are accurately measured in a single crystal $Cu_{68.9}Zn_{31.1}$ by elastic neutron diffraction using ^{65}Cu isotope over a wide reciprocal range[17]. All through the paper the subscript number after the element indicates atomic fraction or percentage and the number before the element is weight percentage. The measured $\alpha_1 = -0.137$ indicates that the element in the cluster center site tends to be nearest-neighbored by the other element, which agree with the negative mixing enthalpy ($\Delta H_{Cu\text{-}Zn} = -6$ kJ/mol)[18]. In accordance with the general cluster formula of binary FCC solid solutions $[A\text{-}M_{12}]A_xB_y$, solute Zn is placed in the cluster center and is nearest-neighbored by $c_1 = 12$ atoms enriched in solvent Cu, leading to cluster formula $[Zn\text{-}Cu_{n1}Zn_{12\text{-}n1}]Zn_xCu_y = [Zn\text{-}M_{12}]Zn_xCu_y$, where M is the averaged nearest-neighbor atom.

First, the number of Cu atoms n_1 in the nearest-neighbor shell is calculated by α_1 following Eq. (3): $n_1 = 0.68\,9{\cdot}12{\cdot}(1 + 0.137) = 9.40$, which is further approximated into roundup integer 10 according to the negative interaction mode between Zn and Cu. Then the chemical unit becomes $[Zn\text{-}Cu_{10}Zn_2]Zn_xCu_y$ with $M = Cu_{10/12}Zn_{2/12}$.

Second, the relationship between x and y is calculated by introducing $R_{Zn/M}$ and $R_{Cu/M}$ into Eq. (2): $1.23x + 0.96y = 4.53$. The Goldschmidt atomic radii[19] are $R_{Zn} = 1.39$ Å and $R_{Cu} = 1.28$ Å, $R_M = (10R_{Cu} + 2R_{Zn})/12 = 1.30$ Å, so that $R_{A/M} = 1.39/1.30 = 1.07$ and $R_{B/M} = 1.28/1.30 = 0.98$. In combination with the alloy composition, $m_B = (10 + y)/(13 + x + y) = 0.689$, the unique ($x$, y) solution is (2.3, 1.8). The close-integers are (2, 2) and (3, 1). The corrosponding chemical units are then $[Zn\text{-}Cu_{10}Zn_2]Zn_2Cu_2 = Cu_{12}Zn_5 = Cu_{70.59}Zn_{29.41} = Cu\text{-}30.01Zn$ (wt.%) and $[Zn\text{-}Cu_{10}Zn_2]Zn_3Cu_1 = Cu_{11}Zn_6 = Cu_{64.71}Zn_{35.29} = Cu\text{-}35.96Zn$. The alloy composition $Cu_{68.9}Zn_{31.1}$ just falls between the two chemical unit compositions. The corresponding mass percentage 64.04–69.99 wt% Cu agrees eactly with the most widely used cartridge brass C26000 (nominal 70Cu–30Zn, with composition ranges specified being 68.5–71.5 Cu, 0.05 Fe max, 0.07 Pb max, 0.15 max other (total), bal Zn)[20].

Cu-8Al aluminum bronze. In $Cu_{85}Al_{15}$, $\alpha_1 = -0.17$ is measured by X-ray diffuse scattering over an angular range from 8° to 60°[21], which leads to $n_1 = 11.93 \approx 12$ and to chemical unit $[Al\text{-}Cu_{12}]Al_xCu_y$. Using $R_{Al} = 1.43$ Å and $R_{Al/Cu} = 1.12$, and complying to the alloy composition, the (x, y) solution is (1.69, 3.23) and the close integers are (2, 3) and (1, 4). The corrosponding chemical unit are $[Al\text{-}Cu_{12}]Al_2Cu_3 = Cu_{15}Al_3 = Cu_{83.33}Al_{16.67} = Cu\text{-}7.83Al$ and $[Al\text{-}Cu_{12}]Al_1Cu_4 = Cu_{16}Al_2 = Cu_{88.89}Al_{11.11} = Cu\text{-}5.04Al$. The mass percentage of Al atoms range from 5.04 to 7.83, which explains the most popular C61000 (92Cu-8Al, with composition ranges being 6.0–8.5 Al, 0.05 Fe max, 0.02 Pb max, 0.20 Zn max, 0.10 Si max, 0.50 max other (total), bal Cu)[20].

Cu-20Ni alloy. In $Cu_{80}Ni_{20}$, the value of α_1, as measured by neutron diffuse scattering using ^{65}Cu isotope, is + 0.058[22], which indicates the tendency of same element neighboring. The number of Cu atoms in the nearest-neighbor shell as calculated using α_1 is 10 and the corresponding chemical unit is $[Cu\text{-}Cu_{10}Ni_2]Cu_xNi_y$. Using $R_{Ni} = 1.25$ Å, the close-integer (x, y) solutions are (2, 1) and (1, 2), which corresponds to the chemical units $[Cu\text{-}Cu_{10}Ni_2]Cu_2Ni_1 = Cu_{13}Ni_3 = Cu_{81.25}Ni_{18.75} = Cu\text{-}17.57Ni$ and $[Cu\text{-}Cu_{10}Ni_2]Cu_1Ni_2 = Cu_{12}Ni_4 = Cu_{75.00}Ni_{25.00} = Cu\text{-}23.54Ni$. The range from 17.57 to 23.54 of Ni atoms explains the alloy C71000 (80Cu-20Ni, specified ranges being 19–23 Ni, 0.05 Pb max, 1.00 Fe, 1.0 Zn max, 1.00 Mn, 0.5 max other (total), bal Cu), which is commonly used as condensers, condenser plates and electrical springs[20].

Exp. alloys at%	α_1	Chemical units	wt% ranges	Alloys specifications
$Cu_{68.9}Zn_{31.1}$	− 0.137	$[Zn\text{-}Cu_{10}Zn_2]Zn_2Cu_2$–$[Zn\text{-}Cu_{10}Zn_2]Zn_3Cu_1$	64.0–70.0 Cu	C26000 (68.5–71.5 Cu) Cartridge brass
$Cu_{85}Al_{15}$	− 0.17	$[Al\text{-}Cu_{12}]Al_2Cu_3$–$[Al\text{-}Cu_{12}]Al_1Cu_4$	5.0–7.8 Al	C61000 (6.0–8.5Al) Aluminum bronze
$Cu_{80}Ni_{20}$	+ 0.058	$[Cu\text{-}Ni_2Cu_{10}]Cu_1Ni_2$–$[Cu\text{-}Ni_2Cu_{10}]Cu_2Ni_1$	17.6–23.5 Ni	C71000 (19–23 Ni)
$Cu_{89.1}Be_{10.9}$	+ 0.077	$[Cu\text{-}Be_1Cu_{11}]Cu_2Be_1$–$[Cu\text{-}Be_1Cu_{11}]Cu_3$	0.9–2.0 Be	C17200 (1.80–2.0 Be) Beryllium bronze
$Ni_{77.5}Fe_{22.5}$	− 0.108	$[Fe\text{-}Ni_{11}Fe_1]Fe_2Ni_1$–$[Fe\text{-}Ni_{11}Fe_1]Fe_1Ni_2$	75.9–82 Ni	K14076 (75–78 Ni)
$Ni_{53.5}Fe_{46.5}$	− 0.077	$[Fe\text{-}Ni_7Fe_5]Fe_2Ni_1$–$[Fe\text{-}Ni_7Fe_5]Fe_1Ni_2$	51.2–57.5 Ni	N14052 (50.5 Ni min)
$Fe_{65}Ni_{35}$	− 0.051	$[Ni\text{-}Fe_9Ni_3]Ni_2Fe_1$–$[Ni\text{-}Fe_9Ni_3]Ni_1Fe_2$	32.3–38.7 Ni	K93601 (35–38)Ni Invar alloy
$Fe_{60}Ni_{40}$	− 0.058	$[Ni\text{-}Fe_8Ni_4]Ni_2Fe_1$–$[Ni\text{-}Fe_8Ni_4]Ni_1Fe_2$	38.7–45.0 Ni	K94490 (43.5–46.5 Ni)
$Fe_{50}Ni_{50}$	− 0.073	$[Ni\text{-}Fe_7Ni_5]Ni_2Fe_1$–$[Ni\text{-}Fe_7Ni_5]Ni_1Fe_2$	45.0–51.2 Ni	K94800 (47–49 Ni)
$Ni_{89}Cr_{11}$	− 0.055	$[Cr\text{-}Ni_{12}]Cr_1Ni_2$–$[Cr\text{-}Ni_{12}]Ni_3$	5.6–11.2 Cr	NCr10 (9.0-10Cr)
$Ni_{80}Cu_{20}$	+ 0.08	$[Ni\text{-}Cu_2Ni_{10}]Ni_2Cu_1$–$[Ni\text{-}Cu_2Ni_{10}]Ni_1Cu_2$	20.0–26.5 Cu	
$Ni_{70}Cu_{30}$	+ 0.118	$[Ni\text{-}Cu_3Ni_9]Ni_1Cu_2$–$[Ni\text{-}Cu_3Ni_9]Ni_2Cu_1$	26.5–33.0 Cu	N04400, (28.0–34.0 Cu) Monel alloy 400
$Ni_{60}Cu_{40}$	+ 0.103	$[Ni\text{-}Cu_4Ni_8]Ni_1Cu_2$–$[Ni\text{-}Cu_4Ni_8]Cu_3$	39.4–45.7 Cu	NCu40-2–1, (38.0–42.0 Cu)

Table 1. Chemical units of typical binary solid-solution-based alloys with FCC structure, derived by combining the measured Cowley's parameter α_1 from Refs.[17,21–26] and the cluster-plus-glue-atom model. The calculated weight percent compositions are comparable to certain alloy specifications. The grades in the table are all ASTM standard UNS numbers, except NCr10 and NCu40-2-1 which are GB/T 5235 standard of China.

Cu-2Be beryllium bronze. In $Cu_{89.1}Be_{10.9}$ alloy, $\alpha_1 = +0.077$, as measured by X-ray diffusion scattering, which is indicative of same-element neighboring[23]. Within the framework of $[Cu\text{-}M_{12}]Cu_xBe_y$, the number of Cu atoms n_1 is 10.79 as calculated from α_1 and is approximated into integer 11. Using $M = Cu_{11/12}Be_{1/12}$ and $R_{Be} = 1.13$ Å, the close-integer (x, y) solution are (2, 1) and (3, 0), leading to chemical units $[Cu\text{-}Cu_{11}Be_1]Cu_2Be_1 = Cu_{14}Be_2 = Cu_{87.50}Be_{12.50} = Cu\text{-}1.99Be$ and $[Cu\text{-}Cu_{11}Be_1]Cu_3 = Cu_{15}Be_1 = Cu_{93.75}Be_{6.25} = Cu\text{-}0.94Be$. This range explains alloy C17200 (1.8 to 2.0 Be, 0.20 Ni + Co min, 0.6 Ni + Co + Fe max, 0.10 Pb max, 0.5 max other (total), bal Cu), which is the most popular Cu-Be alloy for showing high strength and elasticity[20].

It should be stressed that all the above alloy examples refer to the industrial grades the most popularly used in each alloy system. More examples are shown in Table 1, where most of the chemical units explain common industrial specifications. Exceptions are the formulas from alloys $Ni_{80}Cu_{20}$ and $Ni_{60}Cu_{40}$, which indicates that not all formulas correspond to good alloys but the reverse is true: popularly used industrial alloys always satisfy specific cluster formulas as this is required to reach solute homogenization states.

It should be reminded that short-range order parameters such as Cowley's α parameter are sensitive to processing parameters, especially temperature[27]. In principle, the short-range-order parameters should be measured in alloys annealed near the critical temperature where long-range order disappears completely and the atomic distribution tends to be stochastically stable[28,29]. However, the critical temperature is usually unknown in a given alloy. Therefore, the measured α parameters should be more appropriately taken as the tendency along which atoms partition between the nearest-neighbor sites and the next-neighbor glue sites within the molecule-like chemical unit. This is why, for example, Cu-30Zn brass can also be linked to the cluster formula $[Zn\text{-}Cu_{12}]Zn_4$ as we previously proposed[7], which can be regarded as the extreme case when the negative interaction model between Zn and Cu is fully complied, though this formula is equivalent to $[Zn\text{-}Cu_{10}Zn_2]Zn_2Cu_2$ as calculated from the measured α_1.

Finally it should be emphasized that the present work is a combination of our theoretical model with measurable parameters such as the well-established Cowley's α_1. This endeavor strengthens the capability of our model in interpreting alloy compositions. However, the approach developed in the present work cannot be readily extended to multi-component systems (here we confine ourselves to binary systems only), where both the theoretical description and the experimental measurement on short-range ordering are highly difficult. It is noted that, during the last decade, research on short-range ordering is reviving, especially in high-entropy alloys[30–33]. The information provided by sophisticated measuring techniques and by computer simulation will surely enrich our knowledge on chemical short-range ordering. It should be our future goal to use the up-to-date data to deal with composition-complex alloys.

Conclusions

To summarize, after combining the measured short-range-order parameters with our cluster-plus-glue-atom model, we are able to construct molecule-like chemical units which interpret existing industrial alloy composition as specified by standard grades. This work answers the long-standing question on the composition origin of solid-solution-based industrial alloys, by tracing to the molecule-like chemical units implied in chemical short-range ordering in solid solutions.

Data availability

The authors declare that the main data supporting the findings of this study are contained within the paper. All other relevant data are available from the corresponding author upon reasonable request.

Received: 10 September 2021; Accepted: 24 January 2022
Published online: 24 February 2022

References

1. Bruni, G. Solid solutions. *Chem. Rev.* **1**, 345 (1925).
2. Bragg, W. H. The significance of crystal structure. *J. Chem. Soc. Trans.* **121**, 2766–2787 (1922).
3. Bragg, W. L. & Williams, E. J. The effect of thermal agitation on atomic arrangement in alloys. *Proc. R. Soc. Lond. A* **145**, 699–730 (1934).
4. Bethe, H. A. Statistical theory of superlattices. *Proc. R. Soc. Lond. A* **150**, 552–575 (1935).
5. Cowley, J. M. An approximate theory of order in alloys. *Phys. Rev.* **77**, 669–675 (1950).
6. Dong, C. *et al.* From clusters to phase diagrams: Composition rules of quasicrystals and bulk metallic glasses. *J. Phys. D.* **40**, R273 (2007).
7. Dong, D., Wang, Q., Dong, C. & Nieh, T. Molecule-like chemical units in metallic alloys. *Sci. China Mater.* **20**, 1–9 (2021).
8. Jiang, B., Wang, Q., Dong, C. & Liaw, P. Exploration of phase structure evolution induced by alloying elements in Ti alloys via a chemical-short-range-order cluster model. *Sci. Rep.* **9**, 3404 (2019).
9. Harrison, W. *Solid State Theory* (McGraw-Hill, 1970).
10. Friedel, J. Electronic structure of primary solid solutions in metals. *Adv. Phys.* **3**, 446-507 (1954).
11. Friedel, J. Metallic alloys. *Nuovo Cimento* **7**, 287–311 (1958).
12. Häussler, P. Interrelations between atomic and electronic structures-liquid and amorphous metals as model systems. *Phys. Rep.* **222**, 65–143 (1992).
13. Han, G. *et al.* The e/a values of ideal metallic glasses in relation to cluster formulae. *Acta Mater.* **59**, 5917–5923 (2011).
14. Chen, C., Wang, Q., Dong, C., Zhang, Y. & Dong, H. Composition rules of Ni-base single crystal superalloys and its influence on creep properties via a cluster formula approach. *Sci. Rep.* **10**, 21621 (2020).
15. Wen, D. *et al.* Developing fuel cladding Fe-25Cr-22Ni stainless steels with high microstructural stabilities via Mo/Nb/Ti/Ta/W alloying. *Mater. Sci. Eng. A* **719**, 27–42 (2018).
16. Ma, Y. *et al.* A novel soft-magnetic B2-based multiprincipal-element alloy with a uniform distribution of coherent body-centered-cubic nanoprecipitates. *Adv. Mater.* **33**, 2006723 (2021).
17. Reinhard, L., Schönfeld, B., Kostorz, G. & Bührer, W. Short-range order in α-brass. *Phys. Rev. B* **41**, 1727–1734 (1990).
18. Takeuchi, A. & Inoue, A. Classification of bulk metallic glasses by atomic size difference, heat of mixing and period of constituent elements and its application to characterization of the main alloying element. *Mater. Trans.* **46**, 2817–2829 (2005).
19. Gaskell, P. On the density of transition metal-metalloid glasses. *Acta Metall.* **29**, 1203–1211 (1981).
20. Davis, J. R. *ASM Handbook Volume 2: Properties and Selection: Nonferrous Alloys and Special-Purpose Materials* (ASM International, 1998).
21. Kulish, N. & Petrenko, P. Short-range order in binary solid solutions. Ordering and its change on heating in Fe-Al, Cu-Al, and Ag-Al alloys. *Phys. Status Solidi A* **120**, 315–326 (1990).
22. Vrijen, J. & Radelaar, S. Clustering in Cu-Ni alloys: A diffuse neutron-scattering study. *Phys. Rev. B.* **17**, 409–421 (1978).
23. Koo, Y., Cohen, J., Shapiro, S. & Tanner, L. AS-quenched Cu-10.9 at% Be. *Acta Metall.* **36**, 591–604 (1988).
24. Schweika, W. & Haubold, H. Neutron-scattering and Monte Carlo study of short-range order and atomic interaction in $Ni_{0.89}Cr_{0.11}$. *Phys. Rev. B.* **37**, 9240–9248 (1988).
25. Bokoch, S. M. & Tatarenko, V. A. Interatomic interactions in FCC Ni-Fe alloys. *Usp. Fiz. Met.* **11**, 413–450 (2010).
26. Jiang, X., Ice, G. E., Sparks, C. J., Robertson, L. & Zschack, P. Local atomic order and individual pair displacements of $Fe_{46.5}Ni_{53.5}$ and $Fe_{22.5}Ni_{77.5}$ from diffuse x-ray scattering studies. *Phys. Rev. B.* **54**, 3211–3226 (1996).
27. Zhang, R. *et al.* Short-range order and its impact on the CrCoNi medium-entropy alloy. *Nature* **581**, 283–287 (2020).
28. Cowley, J. M. Short-and long-range order parameters in disordered solid solutions. *Phys. Rev.* **120**, 1648–1657 (1960).
29. Sadigh, B. *et al.* Short-range order and phase stability of surface alloys: PdAu on Ru (0001). *Phys. Rev. Lett.* **83**, 1379–1382 (1999).
30. Singh, P., Smirnov, A. V. & Johnson, D. D. Atomic short-range order and incipient long-range order in high-entropy alloys. *Phys. Rev. B.* **91**, 224204 (2015).
31. Chen, X. *et al.* Direct observation of chemical short-range order in a medium-entropy alloy. *Nature* **592**, 712–716 (2021).
32. Singh, R., Sharma, A., Singh, P., Balasubramanian, G. & Johnson, D. D. Accelerating computational modeling and design of high-entropy alloys. *Nat. Comput. Sci.* **1**, 54–61 (2021).
33. Kostiuchenko, T., Ruban, A. V., Neugebauer, J., Shapeev, A. & Krmann, F. Short-range order in face-centered cubic VCoNi alloys. *Phys. Rev. Mater.* **4**, 113802 (2020).

Acknowledgements

The present work was supported by Natural Science Foundation of China (51801017), the Key Discipline and Major Project of Dalian Science and Technology Innovation Foundation (2020JJ25CY004), and by Subject Development Foundation of Key Laboratory of Surface Physics and Chemistry (XKFZ201706).

Author contributions

Z.L. conducted the major calculations and analyzed the alloy data. D.D. and C.D. proposed the theory. S.Z., Q.W., and L.Z. checked the alloy interpretations. All authors participated in writing the paper.

Competing interests

The authors declare no competing interests.

Additional information

Correspondence and requests for materials should be addressed to D.D.

Reprints and permissions information is available at www.nature.com/reprints.

Publisher's note Springer Nature remains neutral with regard to jurisdictional claims in published maps and institutional affiliations.